

A comparative study of acoustic isolation configurations for pMUT array-based applications

Bogdan Vysotskyi, Rachid Haouari, Bart Weekers, Grim Keulemans, Guilherme Brondani Torri, Veronique Rochus

IMEC, Kapeldreef 75, 3001 Leuven, Belgium
bogdan.vysotskyi@imec.be

Abstract

This paper presents an overview of state-of-the-art acoustic isolation in MEMS and compares several acoustic isolation techniques that can be applied to a pMUT array. To keep the solution for acoustic filtering relatively simple in terms of design and fabrication, several typical solutions are considered: use of mesa-type structures, machining ring-shaped pillars of different materials on the surface and combining the trenches etched on the surface with polymer deposited inside it. A direct comparison of these approaches is made using FEM analysis, and it is demonstrated that the crosstalk in pMUT array can be reduced by the value close to the one order of magnitude.

1. Introduction

Acoustic isolation is shown to be of the crucial importance for a variety of commercial MEMS applications, notably for navigation [1], imaging [2] and non-destructive testing (NDT) [3], and even emerging applications such a mid-air haptic feedback [4]. Nevertheless, regarding the importance of the acoustic isolation to reduce the crosstalk between the devices the literature lacks a direct and distinctive comparison of the different techniques for vibration suppression. Present paper performs such a comparison adapted to a pMUT array problematic (such as in [2, 3, 4]) in terms of operating frequencies, dimensions, and materials.

2. Overview of acoustic isolation strategies

For a large number of MEMS systems, including acoustic and inertial, vibrations are known to produce an unwanted device output, reducing the overall quality of the measurement. In a MEMS array configuration, some of the parasitic vibration can be generated by the operating neighboring devices, which is called acoustic crosstalk. Partially these effects can be mitigated by the control electronics and signal processing, but in order to efficiently address the crosstalk, an implementation of an acoustic filter on a chip design-level needs to be considered. In this section, some typical approaches and techniques for vibration suppression are discussed, and their advantages and disadvantages are compared.

As it had been demonstrated in [5] for a semi-infinite solid, surface acoustic waves (SAW) are transferring 67% of the vibration energy, whereas shear (s) waves and pressure (p) waves are responsible for transfer of 26% and 7% of energy, respectively. Thus, addressing SAW propagation may be an efficient strategy for acoustic isolation. In that context, the most simple and direct

solution is to use a mesa-like structure [6], or trenches etched on the surface of the wafer in between the neighboring devices in MEMS array. Originally, this technique had been used to enhance quality factor Q of a dome resonator by redirecting the acoustic waves emitted into the wafer surface back to the device [6]. Conversely, similar type of a mesa structure can be used to suppress acoustic waves produced by neighboring devices in MEMS array. However, such an approach is limited by the operation at very high frequencies (\sim GHz) in the context of MEMS, as far as the mesa placement depends on the wavelength, which is known to be large in solids compared to the typical resonator size. Similar approach is used in building Bragg-type reflectors, however due to the technological reasons it is much easier to use it in vertical acoustic isolation stacks [7], making it very difficult to apply for the array configuration.

The option that is less dependent on operating frequencies is offered by the use of polymer-based materials [8], originally developed for underwater sound absorption. In the polymer-based acoustic dampers, a layer of soft material (that can be structured accordingly as well) is placed on the operating surface, absorbing the vibrational energy present in the system. In terms of crosstalk suppression, the advantage of this technique is its simplicity.

Another interesting group of solutions is the use of metamaterial-based acoustic absorption systems. This type of acoustic isolators is demonstrated to have a high efficiency but known to be difficult to design, miniaturize and fabricate. A typical example of efficient metaplate composed of individual unit cells with a phononic bandgap functioning as an acoustic isolator is demonstrated in [9], where a highly efficient acoustic filtering (\sim 30dB) is reported along 3 axes, with operating frequencies around \sim 20kHz and bandwidth of \sim 5kHz. The significant disadvantage of this type of filtering system is its size – the metaplate occupies around 4cm^2 , making it not very suitable for device array applications. Even more efficient structure with tunable phononic bandgap is reported in [10], but its overall dimension and complexity makes it a suboptimal choice for MEMS applications.

In [11], a solution of building-up a coherent perfect absorber, inspired by optical absorbers, with a use of a Helmholtz resonator as an elementary unit of absorption. A very high absorption values can be achieved theoretically, but such a technique suffers from a unidirectionality and low defect tolerance.

Some truly unique solutions had been reported, such as the development of an omnidirectional acoustic black

hole [12] in a way similar to a gradient index acoustic lens, with outer shell deflecting the acoustic waves and directing them towards the center of a structure, where the vibrations are dissipated. This method has the advantage of a large bandwidth at low operating frequencies (around several kHz), 80% of incident acoustic energy absorption, while the main drawback is relatively large cm-scale size of a system, which makes it unusable for miniaturized systems.

The summary of the existing acoustic isolation techniques in MEMS is presented in the Table 1. It can be seen that various solutions can be used for different frequencies ranges, but not all of them can be miniaturized and, thus, applied to the pMUT array case.

Acoustic isolation type	Typical operating frequencies	Can be easily miniaturized
Mesa structure	~1-10 GHz	Yes
Bragg mirror	~1-10 GHz	No
Polymer-based	1 Hz - 100 kHz	Yes
Metamaterial-based	1 Hz - 10 GHz	No

Table 1. Comparison of acoustic isolation strategies in MEMS

3. Methodology

A typical pMUT device-based array is studied in this paper, and the performance of various acoustic isolation techniques is explored. A schematic on an individual pMUT stack is shown on the Fig. 1. It is composed of two aluminum electrodes covering a piezoelectric AlN layer, and a silicon nitride layer deposited on the top of the stack. A thin void volume is etched on the back side of the stack.



Figure 1: Schematics of an individual MEMS pMUT device

An overall pMUT array schematic is demonstrated on the Fig. 2. It consists of 9 individual MEMS pMUTs, however, for a sake of simplicity a 2D section is made for a series of analyses. A 50µm layer of silicon is added on a backside to simulate an array assembly in context of packaging.

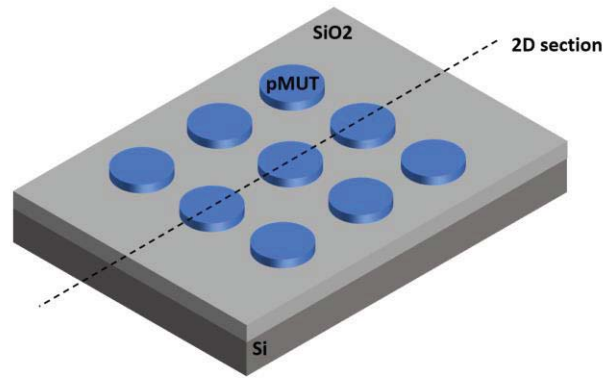


Figure 2: Schematics of a MEMS pMUT array with a section used to build 2D model

A cross section consisting 3 pMUT devices used in Comsol model is depicted on the Fig. 3. The deformation is applied to the central device at resonant frequency simulating the excitation of an operating mode and the deformation on the surface of a neighboring pMUT is evaluated.

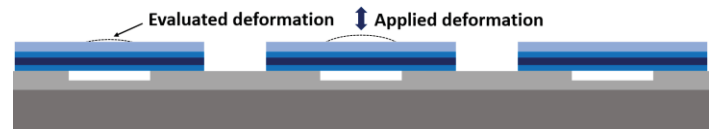


Figure 3: Schematics of a model cross-section used to evaluate crosstalk between neighboring pMUT devices

Several configurations are studied to evaluate the vibration suppression effect with Comsol software in 2D configuration. They are demonstrated on the following figures: mesa-type structure (Fig. 4), ring pillar structure (made of silicon oxide or polymer) (Fig. 8) and a combination of mesa-type structure with deposited polymer layer (Fig. 11). To perform the analysis, a sine excitation force of the same frequency and amplitude is applied to the membrane area on the surface of the device for every configuration. Low reflecting boundary conditions (as defined in Comsol) are applied to the edges of a model to assure the absence of artificial acoustic reflections. A frequency domain study at the first resonant mode (15MHz) is performed at the typical deformation amplitude and the maximum deformation on the neighboring device surface is evaluated. Obtained values are compared to the case where no acoustic isolation solution is applied

4. Results

First, a crosstalk in the array without acoustic isolation is evaluated (configuration from Fig. 3). For a typical central pMUT excitation amplitude of 100nm, the excitation on the neighboring device is evaluated and found to be equal to 2nm. The amplitude of the excitation measured on the neighboring device while the central one

is being excited is referred as a crosstalk amplitude in this paper.

4.1 Mesa-type structure

In this sub-section, mesa-type trench structure (demonstrated on the Fig. 4) is evaluated in terms of acoustic crosstalk reduction. The structure is not expected to be as efficiently as in [6] as far as a $\lambda/4$ inter device placement cannot be respected due to the high acoustic wavelength in silicon at operating frequency.

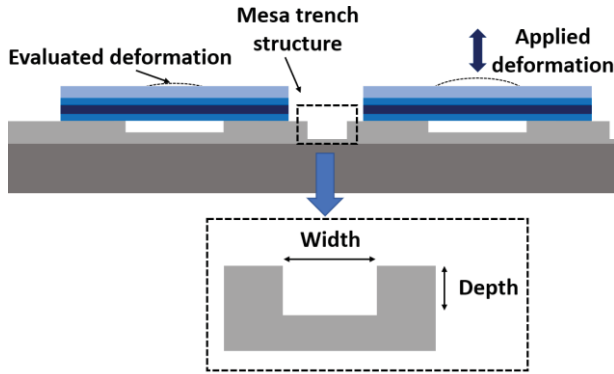


Figure 4: Schematics of a mesa-type trench structure used for an acoustic crosstalk reduction

The results of a crosstalk dependence on a mesa depth with fixed width is shown on the Fig. 5. It can be seen that an optimal point which minimizes a coupling amplitude can be found around 2.5 μm .

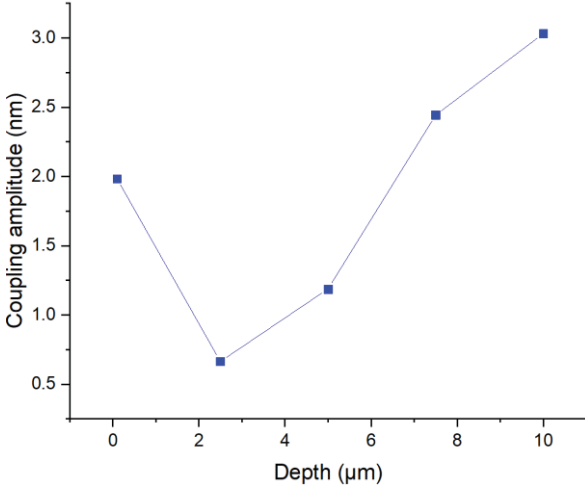


Figure 5: Simulated result of a coupling amplitude as a function of depth of mesa trenches with fixed width of 10 μm

Conversely, the impact of mesa width on a crosstalk with fixed depth is depicted on the Fig. 6. This result is different from the previous one and demonstrates that higher width of mesa trench is preferred.

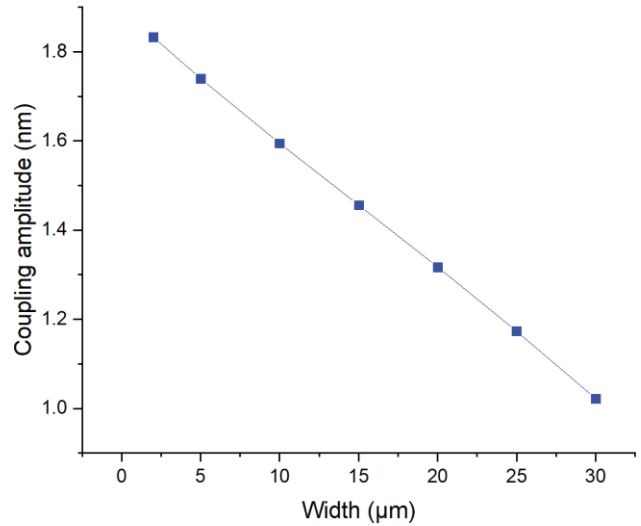


Figure 6: Simulated result of a coupling amplitude as a function of width of mesa trenches with fixed depth of 1 μm

A series of simulations are carried out to evaluate the optimal parameters of mesa trenches dimensions. The results are plotted on the color map on Fig. 7. It has a saddle shape which demonstrates the relation between width and depth impact, with a minimum value of coupling amplitude found to be 0.23nm with trench width of 20 μm and depth of 2.5 μm . This result demonstrates that mesa structure can remove up to 89% of crosstalk according to this result.

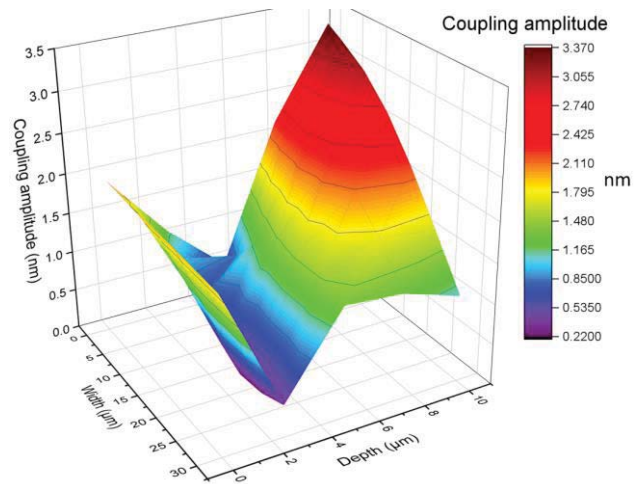


Figure 7: Simulated result of a coupling amplitude as a function of width and depth of mesa trenches

4.2 Ring-shaped pillars

A simple surface ring-shaped pillar structure is analyzed. It is depicted on the Fig. 8. Two cases are considered: silicon oxide pillars machined on the top layer and polymer pillars deposited on the surface.

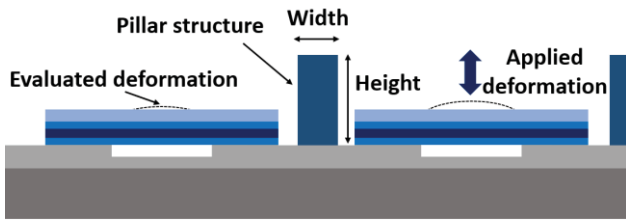


Figure 8: Cross-section schematics of a pillar ring-shaped structure used for an acoustic crosstalk reduction

4.2.1 Silicon oxide pillars

As in the previous sections, a series of simulations is performed to evaluate the coupling amplitude as a function of width and height of silicon oxide pillars. The results are depicted on the Fig. 9. It can be seen that an optimal configuration exists and corresponds to the pillar height of $20\mu\text{m}$ and width of $15\mu\text{m}$ with an evaluated coupling amplitude of 0.44nm , which corresponds to the overall improvement in a crosstalk amplitude reduction of 78%.

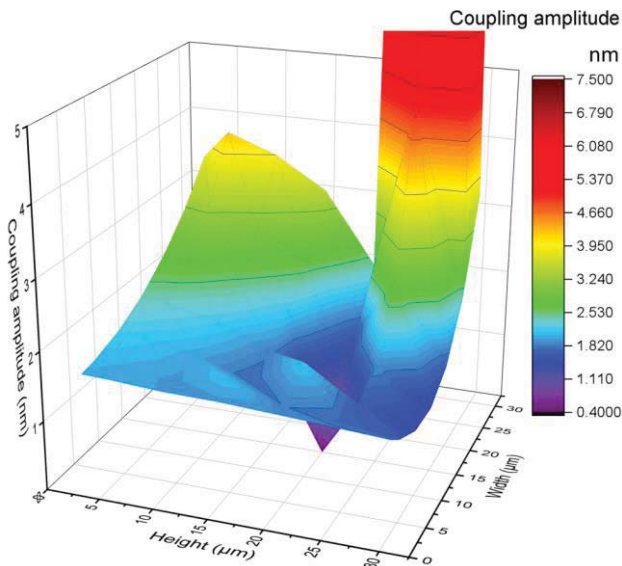


Figure 9: Simulated result of a coupling amplitude as a function of width and height of silicon oxide pillars etched on the top of the wafer

4.2.2 Polymer pillars

In this case, the pillars are considered to be formed by a polymer deposited on the surface of the wafer. As previously, the study of height and width impact is carried out. The results are shown on the Fig. 10. It can be seen that this acoustic crosstalk reduction solution is not very efficient: the minimal coupling amplitude is found to be equal to 1.84nm , which corresponds to 8% of crosstalk amplitude reduction.

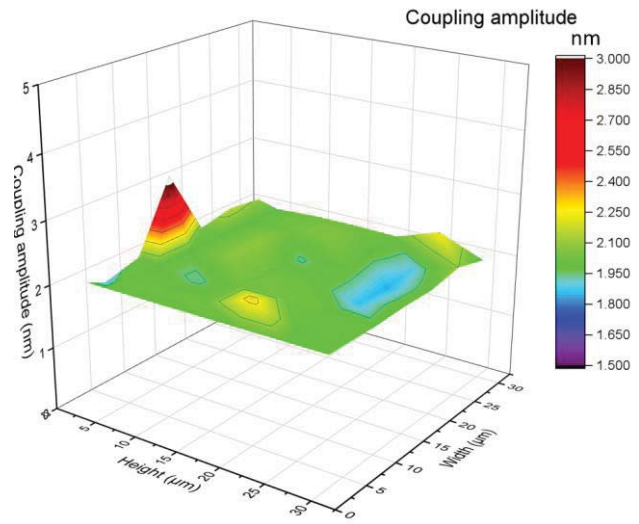


Figure 10: Simulated result of a coupling amplitude as a function of width and height of polymer pillars deposited on the top of the wafer

4.3 Mesa-type structure with trenches filled with polymer

Finally, in this section a combination of two solutions is considered. A schematic cross-section of this configuration is depicted on Fig. 11.

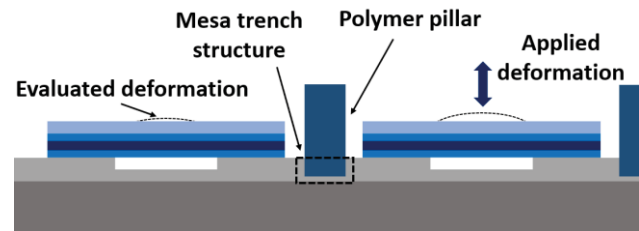


Figure 11: Cross-section schematics of a mesa-type structure with trenches filled with polymer used for an acoustic crosstalk reduction

The results of mesa-type structure with trenches filled with polymer dimensions analysis are plotted on the Fig. 12. The pillar height is fixed at the value of $5\mu\text{m}$. It can be seen that this result is very similar to the one obtained in the section 4.1, and demonstrates that polymer structures are not efficient at acoustic crosstalk reduction in studied problem. Similar to the simple mesa structure, the evaluated optimal value is 0.24nm for a crosstalk amplitude with mesa width of $20\mu\text{m}$ and depth of $2.5\mu\text{m}$, with the crosstalk reduction efficiency estimated to be equal to 88%.

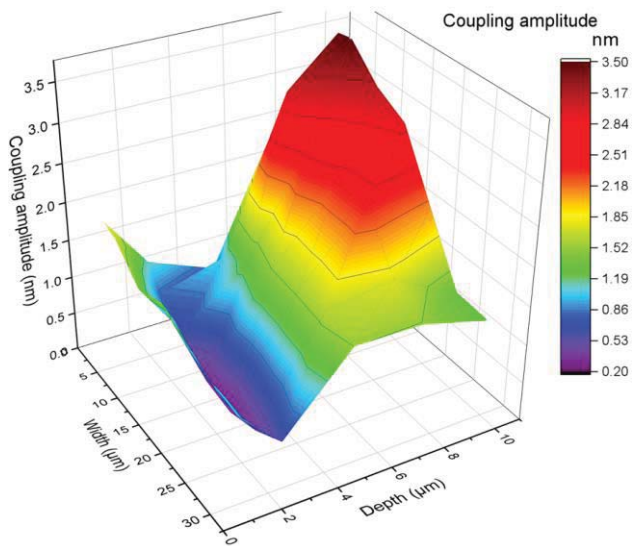


Figure 12: Simulated result of a coupling amplitude as a function of mesa width and depth, with trenches filled with polymer

5. Conclusions

This paper presents a general overview of the modern techniques used to introduce the acoustic isolation in the MEMS-based systems. A general overview of modern techniques for acoustic isolations in MEMS is presented and compared in terms of their applicability to pMUT arrays in terms of their operating frequencies, miniaturizability and crosstalk reduction efficiency.

Several solutions that can be applied to a typical existing pMUT design are considered: mesa-type structure, depositing of polymer ring-shaped pillars and using an additional polymer layer on the back side of the system. These results are compared to the reference case where no acoustic isolation is present. These numerical findings are summarized at Table 2. From presented study it can be concluded that a mesa-type structure, while being relatively simply to design and fabricate, may provide an optimal design solution to reducing the crosstalk by almost one order of magnitude.

Filter configuration	Crosstalk amplitude, nm	Crosstalk reduction
No acoustic isolation	2	0%
Mesa-type structure	0.23	89%
Silicon oxide pillars	0.44	78%
Polymer pillars	1.84	8%
Combined solution (Mesa-type + polymer)	0.24	88%

Table 2. Results summary for different acoustic isolation configurations for pMUT array applications

References

1. A. Efimovskaya et al., "On cross-talk between gyroscopes integrated on a folded MEMS IMU Cube", IEEE 30th International Conference on Micro Electro Mechanical Systems (MEMS), 2017;
2. Y. Yang et al., "An Ultra-High Element Density pMUT Array with Low Crosstalk for 3-D Medical Imaging", Sensors, 13(8), 9624-9634, 2013;
3. T. Xu et al., "Array Design of Piezoelectric Micromachined Ultrasonic Transducers With Low-Crosstalk and High-Emission Performance", IEEE Transactions on Ultrasonics, Ferroelectrics, and Frequency Control, Volume: 67, Issue: 4, 2020;
4. A. Halbach et al., "Display Compatible PMUT Array for Mid-Air Haptic Feedback", 20th International Conference on Solid-State Sensors, Actuators and Microsystems & Eurosensors XXXIII (TRANSDUCERS & EUROSENSORS XXXIII), 2019;
5. G. Miller et al., "On the partition of energy between elastic waves in a semi-infinite solid", Proc. R. Soc. Lond. A, Math. Phys. Sci., Vol. 233, pp. 55–69, 1955;
6. M. Pandey et al., "Reducing Anchor Loss in MEMS Resonators Using Mesa Isolation", Journal Of Microelectromechanical Systems, Vol. 18, No. 4, 2009;
7. A. Zazerin et al., "Bragg reflector acoustic impedance RLC model", ElectronComm, Vol. 20, 2015;
8. Y. Fu et al., "A review on polymer-based materials for underwater sound absorption", Polymer Testing, Vol. 96, 107115, 2021;
9. Z. Yao et al., "Design, Fabrication and Experimental Validation of a Metaplate for Vibration Isolation in MEMS", Journal Of Microelectromechanical Systems, 2020;
10. L. D'Alessandro et al., "3D auxetic single material periodic structure with ultra-wide tunable bandgap", Scientific Reports, Vol. 8, 2262, 2018;
11. P. Wei et al., "Symmetrical and anti-symmetrical coherent perfect absorption for acoustic waves", Applied Physics Letters 104, 121902, 2014;
12. A. Climente et al., "Omnidirectional broadband acoustic absorber based on metamaterials", Applied Physics Letters 100, 144103, 2012.